

Received January 12, 2018; reviewed; accepted February 27, 2018

Flotation kinetics and thermodynamic behavior of chalcopyrite and pyrite in high alkaline systems

Huashan Yan ^{1,2}, Qinzhi Yuan ^{1,2}, Liping Zhou ¹, Tingsheng Qiu ^{1,2}, Guanghua Ai ^{1,2}

¹ College of Resource and Environmental Engineering, Jiangxi University of Science and Technology, Ganzhou 341000, China

² Jiangxi Key Laboratory of Mining Engineering, Ganzhou 341000, China

Corresponding author: qiutingsheng@163.com (Tingsheng Qiu), 9120050022@jxust.edu.cn (Guanghua Ai)

Abstract: The monomineral flotation test and microcalorimetry were used to study the flotation kinetics and thermodynamic behavior of chalcopyrite and pyrite in high alkaline systems of lime and NaOH. The results showed that in these systems there were less hydrophilic substances on the chalcopyrite surface, so that the apparent activation energy of sodium butyl xanthate (SBX) adsorption on chalcopyrite surface was low. This promoted the adsorption of SBX and increased the flotation rate and recovery of chalcopyrite. In contrast, the hydrophilic $\text{Fe}(\text{OH})_3$ and SO_4^{2-} formed by oxidation on the pyrite surface increased the adsorption activation energy of SBX. Thus, the flotation rate and recovery of pyrite were lower. Moreover, in the lime high alkaline system, the hydrophilic calcium film generated on the pyrite surface further hindered the adsorption of SBX, thereby further inhibiting pyrite in this environment. In other words, the lime high alkaline environment increased the apparent activation energy difference of SBX adsorption between chalcopyrite and pyrite compared to the NaOH system, facilitating the flotation separation of chalcopyrite and pyrite. The results can help with the theoretical research of flotation separation of other minerals, and provide guidance for developing low alkaline and lime-free pyrite depressants.

Keywords: Chalcopyrite, pyrite, high alkaline, flotation kinetics, microcalorimetry, flotation separation

1. Introduction

In China, copper is mainly produced from chalcopyrite. Since it is generally in a symbiotic combination with pyrite, chalcopyrite needs to be separated from pyrite by flotation, which is usually referred to as the separation of copper and sulfur. To improve the separation efficiency, some scholars have studied the flotation kinetics (Qiu et al., 2016) and electrochemistry (Ekmekçi and Demirel, 1997; He et al., 2006; Owusu et al., 2013) of chalcopyrite and pyrite. The adsorption of some collectors on the surfaces of chalcopyrite and pyrite also has been analyzed (Montalti et al., 1991; Sun et al., 2010; Zhang et al., 2013). Other researchers investigated the impact of grinding conditions (Chen and Peng, 2015; Peng et al., 2003), pulp filling (Owusu et al., 2015), pyrite content (Owusu et al., 2014), and microwave irradiation treatment (Elmahdy et al., 2016) on the flotation separation of chalcopyrite and pyrite. In practice, the key of flotation separation of these two minerals is the addition of pyrite depressants (Leppinen, 1990; Fuerstenau et al., 1985). At present, the most widely used flotation separation process involves the addition of a lot of lime in the pulp to inhibit sulfur and float copper in a high alkaline environment. This technology is quite mature, and the separation effect is good. However, such high alkaline environment causes several problems, such as scaling and blockage, easy corrosion of equipment, serious pollution in the wastewater, and unfavorable comprehensive recovery of valuable associated components (Boulton et al., 2001; Shen et al., 1998). Therefore, it is of great theoretical and practical significance to find efficient pyrite depressants for flotation separation in a low alkaline environment without lime, and to improve the comprehensive utilization of mineral resources. To this end,

understanding the mechanism of pyrite flotation inhibition in the high alkaline environment will help guide the development of low alkaline pyrite depressants.

The inhibition mechanism of lime on pyrite flotation has been extensively studied. Li et al. (2007) calculated the electronic structure and surface energy density distribution of pyrite (100) surface, and found that the surface easily adsorbed OH^- and $\text{Ca}(\text{OH})^+$ in the lime system and blocked the adsorption of xanthate (a collector). Based on the electrochemical mechanism of the inhibition of sulfide ore flotation, Woods (2003) and Sun et al. (2010) considered that the high alkali environment decreases the surface oxidation potential of pyrite, thereby promoting its surface oxidation to produce hydrophilic substances such as $\text{Fe}(\text{OH})_3$. Li et al. (2007) studied the electrochemical behavior of xanthate on the surface of pyrite and the influence of lime system on it by cyclic voltammetry. It was pointed out that xanthate was difficult to adsorb onto the pyrite surface under lime system and easily oxidized to form dixanthogen. Using the electrochemical regulation band model of sulfide ore, Chen et al. (2000) considered that the high alkali condition will change the edge energy of the pyrite and facilitate its oxidation. According to the X-ray photoelectron spectroscopy (XPS) analysis, some hydrophilic substances such as CaSO_4 , $\text{Ca}(\text{OH})_2$, and $\text{Fe}(\text{OH})_3$ exist on the surface of pyrite under high alkaline and high calcium conditions (Qin et al., 1996; Murphy and Strongin, 2009). Zhang et al. (2011) studied the electrochemical behaviors of pyrite flotation using lime and sodium hydroxide (NaOH) as depressants, and pointed out that the paraffin reaction resistance of pyrite surface decreases with increasing pH value, which enhances the electron transport on pyrite surface and makes the surface easier to oxidize. The presence of the calcium film in the lime system leads to a higher increase in Faraday reaction resistance than that in the NaOH system. In summary, the mechanism of pyrite depressants was either to desorb the collector or activator from the pyrite surface, deactivate the activating ions, prevent collector adsorption on pyrite, or make the pyrite surface hydrophilic (Wark and Cox, 1934; Gaudin, 1957; Janetski et al., 1977; Fornasiero et al., 1992; Chen et al., 2011; Li et al., 2012; Mu et al., 2016).

While the inhibition mechanism of pyrite flotation in high alkaline environment with lime is relatively clear, the effects of different alkaline environments on the flotation behavior of chalcopyrite and pyrite are poorly understood. Therefore, in this study, we will compare the flotation behavior of chalcopyrite and pyrite in high alkaline environments with lime or NaOH from the perspectives of kinetics and thermodynamics. The goal was to explain the internal mechanism of copper and sulfur flotation separation in these high alkaline environments. The results can provide references for the theoretical research of flotation separation of other minerals, and help developing low alkaline and lime-free pyrite depressants.

2. Experiments

2.1 Materials and reagents

The monominerals of chalcopyrite and pyrite were obtained from a mine in Jiangxi Province, China, with the respective purity of 98.58% and 98.91%. Their X-ray diffraction (XRD) spectra are shown in Fig. 1. Sodium butyl xanthate (SBX) with a purity of more than 95% was synthesized in the laboratory. H_2SO_4 , NaOH, and lime (all analytical grade) and 2# oil (industrial grade) were purchased from Sinopharm Chemical Reagent Company (Shanghai, China).

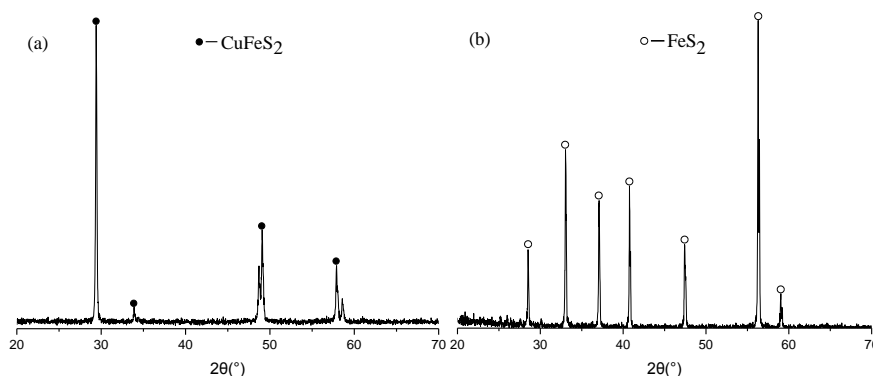


Fig. 1. XRD spectra of chalcopyrite and pyrite

2.2 Flotation tests

The flotation test was carried out in a 40-cm³ plexiglass cell of a XFG-II flotation machine (Jilin Prospecting Machinery Factory, China). For each test, 2.0 g of the sample was washed ultrasonically and placed in the flotation cell. Distilled water, pH regulator, collector, and frother were added in turn, and the conditioning time after each addition was 1.0, 2.0, 3.0, and 2.0 min, respectively. Then, 4.0 min of artificial scraping was carried out. The foam concentrates and tailings in the cell were filtered, dried, and weighed to calculate the recovery according to the mass percentage. Each flotation test was repeated three times, and the reported values are the averages.

2.3 Microcalorimetry tests

A microcalorimeter can be used to continuously and accurately monitor micro energy changes in a reaction process. The recorded calorimetric curves could simultaneously provide in-situ thermodynamic and kinetic information in real time and losslessly (Yang et al., 2014). At present, microcalorimetry is widely used in chemical engineering, biochemistry, physical chemistry, organic chemistry, and many other fields. However, there are only a few reports of its application in mineral processing. Several research groups used it to investigate the adsorption of collectors on mineral surfaces (Chen et al., 2013; Haung and Miller, 1978; Lan et al., 2016; Maier et al. 1997; Mellgren, 1966) and the dissolution of several minerals (Chen et al., 2007; Liu et al., 2002). Some thermodynamic and kinetic parameters were also determined.

In this study, the calorimetric measurements were carried out at 298.15, 301.15, and 304.15 K with an RD496-2000 type microcalorimeter (Mianyang Zhongwu Thermal Analysis Instrument, China), with the respective calorimetry constants of 6.667×10^{-2} , 6.638×10^{-2} and $6.627 \times 10^{-2} \text{ V} \cdot \text{W}^{-1}$. The measurement portion of the microcalorimeter is composed of two identical thermopiles placed in the measuring and reference cells in order to minimize interference. The difference in thermal effect between the two cells was taken as that of the reaction process. The schematic diagram of the measuring cell is shown in Fig. 2, and its preparation steps are as follows. Firstly, 0.03 g mineral sample and 1.0 mL of NaOH or lime solution (pH = 12) were put into the outer glass tube. A given amount of SBX solution, whose concentration was determined by flotation test, was put into an inner glass tube. Then, the inner glass tube was put into the outer one; and together they were put into a stainless-steel pipe, covered with a perforated upper end cap, and secured using a circlip for a hole. Next, the steel needle with a press handle and spring was inserted into the hole of the perforated upper end cap, until the tip was about to touch the bottom of the inner tube. The reference cell was prepared identically, except there was no mineral sample in the outer tube. This ensured that the thermal interference from other processes, such as the dilution of collector solution, rupture of glass tube, and mixing of two solutions could be eliminated.

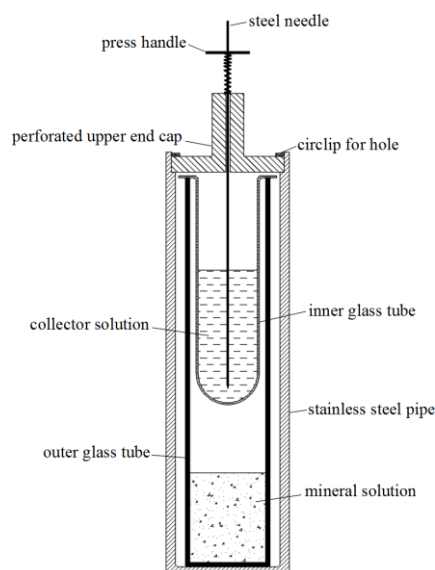


Fig. 2. Schematic diagram of the measuring cell

After the measuring and reference cells were placed in the furnace body, the temperature of the laboratory was kept constant at 273.15 K, and the calorimetric parameters were set by the control software. When the baseline was stable, the steel needles in the two cells were pushed down quickly at the same time to pierce the inner tubes. This starts the adsorption process of SBX on the mineral surface. At the same time, the difference in thermal effect between the two cells was converted from a thermal signal into an electrical signal by the measurement and control instrument, and the calorimetric curve was recorded on the computer in real time.

3. Results and discussions

3.1 Effects of NaOH and lime on flotation behavior of chalcopyrite and pyrite

During mineral flotation, H_2SO_4 is generally used as an acidic pH regulator, and NaOH or lime as an alkaline pH regulator. The current study examines the effects of NaOH and lime on the flotation behavior of chalcopyrite and pyrite. In the flotation test, SBX with a concentration of 0.1 mol m^{-3} was used as collector, H_2SO_4 and NaOH or lime were used as pH regulators, and $1 \times 10^4 \text{ mg m}^{-3}$ of 2# oil was used as the frother.

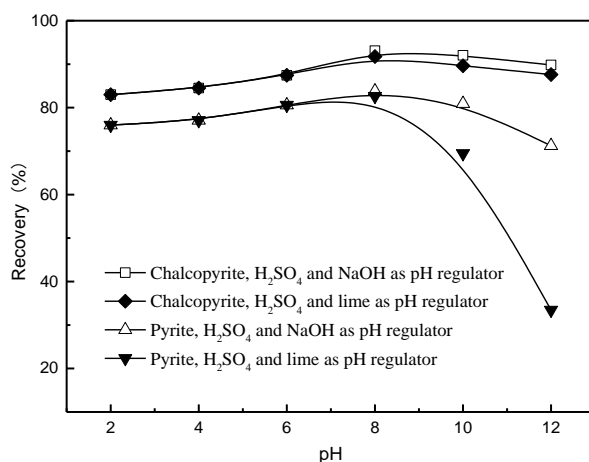
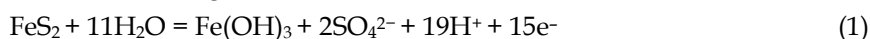


Fig. 3 Effects of pH regulators on the flotation of chalcopyrite and pyrite

As shown in Fig. 3, both chalcopyrite and pyrite exhibited their optimum floatability in a neutral pulp environment. Because of the partial decomposition of xanthate, the floatability of these two minerals in acidic environment is slightly worse. In the alkaline environments of lime and NaOH, chalcopyrite has good floatability, and its recovery only slightly decreases with the increase of pH. Meanwhile, the recovery of pyrite obviously decreases with the increase of pH. Moreover, when lime is used as the regulator, the flotation recovery of pyrite shows a larger reduction than that when using NaOH. This indicates that pyrite flotation is inhibited in both of the alkaline environments, but more so in lime solution than in NaOH solution.

In an alkaline environment, the following oxidation reaction occurs on pyrite surface (Leppinen, 1990; Zhang et al., 2011; Moslemi and Gharabaghi, 2017):



Due to the production of H^+ , the reaction becomes more favorable with the increase of pH. Thus, larger amounts of hydrophilic $Fe(OH)_3$ and SO_4^{2-} are formed on the surface of pyrite, reducing the floatability. In the high alkaline environment with lime, hydrophilic substances such as $CaSO_4$ and $Ca(OH)_2$ are formed on the pyrite surface due to the presence of free calcium oxide, further strengthening the inhibition of pyrite (Fuerstenau et al., 1985; Hu et al., 2000; Rao and Leja, 2004; Li et al., 2012). Therefore, when the pulp pH is adjusted by H_2SO_4 and NaOH, the difference in recovery between chalcopyrite and pyrite is small in the whole pH range, which is unfavorable for their flotation separation. In contrast, when using H_2SO_4 and lime, the difference in recovery increases rapidly with the increase of pH, allowing the effective flotation separation of chalcopyrite and pyrite in lime high alkaline environment.

3.2 Flotation kinetics of chalcopyrite and pyrite in high alkaline environments of NaOH and lime

We propose a kinetic mechanism to explain the flotation behavior of chalcopyrite and pyrite in the high alkali environments of NaOH and lime. When the pulp pH was adjusted to 12 using NaOH or lime using SBX (0.1 mol m^{-3}) as collector and 2# oi ($1 \times 10^4 \text{ mg m}^{-3}$) as frother, flotation tests were carried out for chalcopyrite and pyrite at the flotation times of 0.2, 0.4, 1.0, 2.0, 3.0, and 4.0 min. The results are shown in Table 1.

Table 1. Effect of flotation time on recovery of chalcopyrite and pyrite

Flotation time / min	0.2	0.4	1.0	2.0	3.0	4.0
Chalcopyrite recovery (pH=12, NaOH) / %	26.58	44.69	70.03	83.05	87.61	89.82
Pyrite recovery (pH=12, NaOH) / %	14.64	25.14	46.54	61.67	68.71	72.25
Chalcopyrite recovery (pH=12, lime) / %	24.16	42.34	62.03	75.15	85.11	87.62
Pyrite recovery (pH=12, lime) / %	5.12	9.51	19.03	27.56	31.33	33.45

The obtained data were fitted to Eqs. (2)–(4) (Bayat et al., 2004; Chaves and Ruiz, 2009; Zhang et al., 2013). Nonlinear curve fitting was carried out by using Marquardt and universal global optimization methods in the 1st Opt software package, and the result is shown in Fig. 4.

$$\varepsilon = \varepsilon_{\infty}[1 - \exp(-kt)] \quad (2)$$

$$\varepsilon = \varepsilon_{\infty}\left\{1 - \frac{1}{kt}[1 - \exp(-kt)]\right\} \quad (3)$$

$$\varepsilon = \frac{\varepsilon_{\infty}^2 kt}{1 + \varepsilon_{\infty} kt} \quad (4)$$

where ε is the predicted recovery, ε_{∞} is the theoretical recovery, k is the flotation rate constant and t is the time.

For chalcopyrite/NaOH, chalcopyrite/lime, and pyrite/NaOH systems, model (2) produced the best fitting results, with the respective R^2 values of 0.9999, 0.9911, and 0.9999. For the flotation test data of pyrite/lime system, model (1) produced the best fit ($R^2 = 0.9999$). The calculated flotation kinetic parameters of chalcopyrite and pyrite are given in Table 2.

Table 2. Flotation kinetic parameters of chalcopyrite and pyrite

Flotation kinetic parameters	$\varepsilon_{\infty} / \%$	$\Delta\varepsilon_{\infty} / \%$	k	Δk
Chalcopyrite/ pH=12/ NaOH	95.00	12.32	3.67	1.71
Pyrite/ pH=12/ NaOH	82.68		1.96	
Chalcopyrite/ pH=12/ lime	93.47	52.73	3.08	2.29
Pyrite/ pH=12/ lime	40.74		0.79	

In these two high alkaline systems, the values of ε_{∞} and k are ranked as chalcopyrite/NaOH > chalcopyrite/lime > pyrite/NaOH > pyrite/lime. The flotation kinetic parameters of chalcopyrite in the two environments are close, while those of pyrite in lime system are much lower than for other conditions. This is consistent with their predicted floatability in the corresponding environments.

In addition, in the NaOH system, the differences of flotation kinetic parameters between chalcopyrite and pyrite are $\Delta\varepsilon_{\infty} = 12.32\%$ and $\Delta k = 1.71$. In the lime high alkaline system, these values are raised to 52.73% and 2.29, respectively. This is consistent with the flotation test results, and explains the reason why chalcopyrite and pyrite can be effectively separated in lime high alkaline environment, from the kinetics point of view.

3.3 Thermodynamic analysis of the surface adsorption of SBX on chalcopyrite and pyrite

According to the method described in Section 2.3, the calorimetric test was carried out using SBX with a concentration of 0.1 mol m^{-3} . The calorimetric curves of the adsorption of SBX on the two mineral surfaces in high alkaline environments of NaOH and lime are shown in Fig. 5. The time axis represents the time of the adsorption process, the heat flow axis represents the instantaneous heat magnitude, and the integrated area under the calorimetric curve represents the total calories released in the whole

adsorption process (i.e., the heat of adsorption). A positive calorimetric curve represents an exothermic process, and a negative curve an endothermic process.

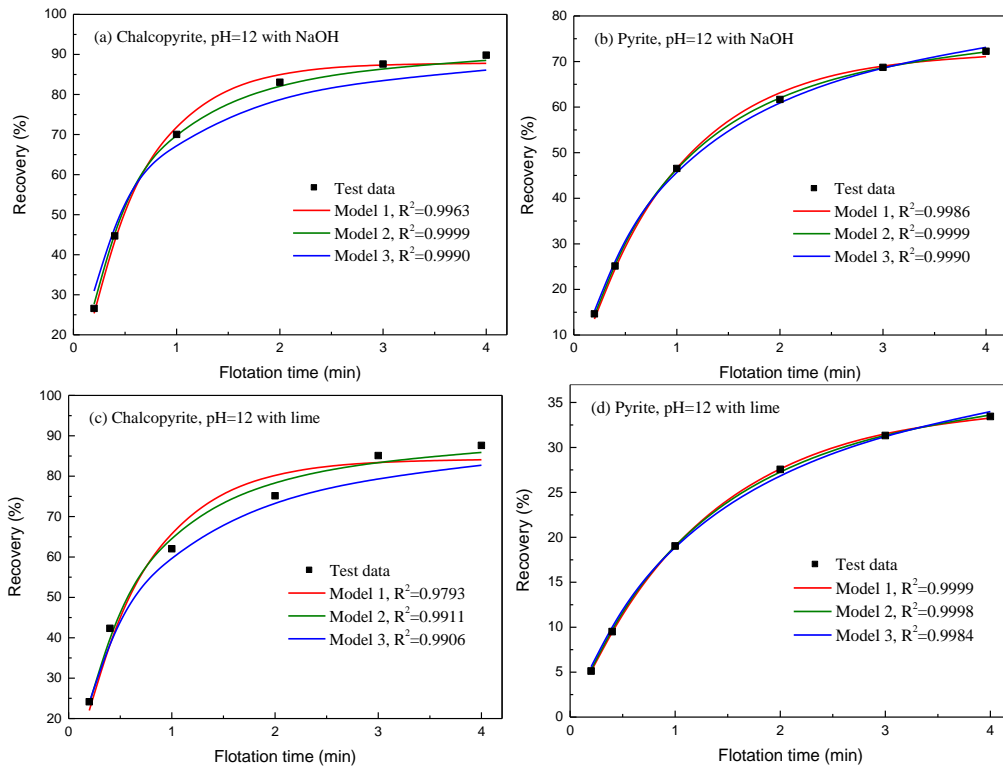


Fig. 4 Fitted curves for chalcopyrite and pyrite flotation kinetics

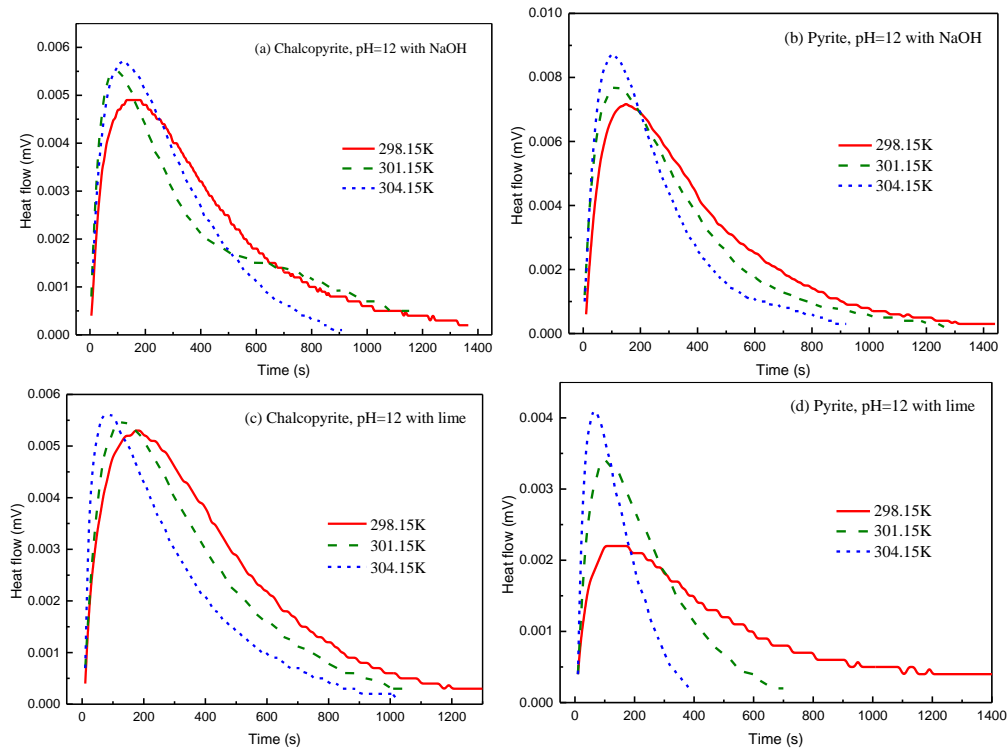


Fig. 5 Calorimetric curves of the adsorption of SBX on the surfaces of chalcopyrite and pyrite

All the calorimetric curves in Fig. 5 are positive, therefore the adsorption of SBX is exothermic for both minerals. At higher temperatures, the adsorption of SBX becomes faster, meaning that the

adsorption rate becomes faster. At the same time, the area under the calorimetric curve is reduced, i.e. with a lower heat of adsorption. This is consistent with the nature of exothermic reactions.

According to the method described in the literature (Gao et al., 2002), the calorimetric curves were treated by software, and the thermodynamic parameters were calculated by the least square method on the basis of Eqs. (5) and (6). The results are shown in Table 3.

$$\ln\left(\frac{1}{H_\infty} \cdot \frac{dH_t}{dt}\right) = \ln k + n \ln\left(1 - \frac{H_t}{H_\infty}\right) \quad (5)$$

$$\ln k = \ln A - \frac{E_a}{RT} \quad (6)$$

where H_∞ is the gross thermal value produced by reaction; t is the reaction time; H_t is the thermal value produced by reaction in t time; dH_t/dt is the enthalpy change rate at t time; k is the reaction rate constant; n is the reaction order; $\ln A$ is the pre-exponential factor; E_a is the apparent activation energy; R is the molar gas constant; T is the measured temperature.

Table 3. Thermodynamic parameters of the adsorption of SBX on the surfaces of chalcopyrite and pyrite

Systems	T / K	Q / mJ	$\ln A / s^{-1}$	$E_a / kJ \cdot mol^{-1}$	R^2	$\Delta E_a / kJ \cdot mol^{-1}$
Chalcopyrite/ pH=12/ NaOH	298.15	40.17	8.61	36.17	0.992	27.27
	301.15	36.87				
	304.15	33.73				
Pyrite/ pH=12/ NaOH	298.15	55.82	19.66	63.44	0.974	
	301.15	50.52				
	304.15	43.64				
Chalcopyrite/ pH=12/ lime	298.15	44.14	11.92	44.40	0.998	107.57
	301.15	37.41				
	304.15	31.15				
Pyrite/ pH=12/ lime	298.15	22.64	55.16	151.97	0.998	
	301.15	16.24				
	304.15	11.39				

In Table 3, Q is the adsorption heat, that is, H_∞ , and R^2 is the correlation coefficient. The adsorption heat decreases at higher temperatures under each condition, which verifies the regularity of the calorimetric curve. The correlation coefficients under all conditions are close to 1.0, indicating that the calculated pre-exponential factor and apparent activation energy values are accurate and reliable. The adsorption heat of SBX on the surface of pyrite in lime high alkaline environment is obviously lower than those of the other conditions. This should be attributed to the hydrophilic substances generated on the surface of pyrite, such as $CaSO_4$ and $Ca(OH)_2$, which weakens the adsorption of SBX.

The activation energy can be used to characterize the difficulty of a reaction: a lower activation energy indicates that the reaction is easier to proceed. From Table 3, the apparent activation energy can be ranked as chalcopyrite/NaOH < chalcopyrite/lime < pyrite/NaOH < pyrite/lime, with the adsorption becoming progressively more difficult. The last apparent activation energy (pyrite surface in lime high alkaline environment) is much higher than the rest, meaning that this adsorption process is a lot more difficult. In addition, the trend of the thermodynamic parameters is consistent with that of flotation recovery and kinetic parameters. This is because the more easily the mineral surface adsorbs the collector, the higher the flotation recovery and flotation rate.

The apparent activation energies of SBX adsorption on chalcopyrite and pyrite in lime high alkaline system differ by 107.57 $kJ \cdot mol^{-1}$, which is much larger than their difference of 27.27 $kJ \cdot mol^{-1}$ in NaOH high alkaline system. Maybe this can explain why their flotation separation is more effective in the lime system than that in the NaOH system from the thermodynamic point of view.

4. Conclusions

1). The monomineral flotation and associated kinetic data show that the flotation of chalcopyrite was not inhibited in NaOH or lime high alkaline environments, therefore faster flotation rate and higher recovery were obtained. In contrast, pyrite was subject to strong inhibition in these systems, leading to much lower flotation rate and theoretical recovery. Due to the presence of hydrophilic calcium film, the

floatability of pyrite in the lime environment was much lower than that in NaOH environment, and the flotation rate and theoretical recovery were the lowest. In lime high alkali environment, the difference in flotation rate between pyrite and chalcopyrite was the largest, which is most beneficial to their flotation separation.

2). The obtained thermodynamic data show that, in the NaOH and lime high alkaline environments, the lower apparent activation energy means that SBX more easily adsorbs on the surface of chalcopyrite and gives it good floatability. On the other hand, due to the presence of hydrophilic substances such as $\text{Fe}(\text{OH})_3$, SBX adsorption on the surface of pyrite has a higher apparent activation energy, meaning more difficult adsorption and lower floatability of pyrite. Moreover, in the lime environment, hydrophilic CaSO_4 and $\text{Ca}(\text{OH})_2$ can form on the pyrite surface, making the adsorption of SBX even more difficult. Therefore, pyrite flotation is most strongly inhibited in this environment. Since the activation energy difference between the minerals is the highest under the lime environment, this high alkaline environment is more conducive to the flotation separation of chalcopyrite and pyrite.

Acknowledgment

This work was financially supported by the Projects of National Natural Science Foundation of China [grant number 51474114, 51564014 and 51504105], Key Research and Development Plan of Jiangxi Province [grant number 20171BBG70043], Jiangxi Natural Science Foundation [grant number 20171BAB206025], and the Program for Excellent Young Talents, JXUST, China.

References

- BAYAT, O., UCURUM, M., POOLE, C., 2004. *Effects of size distribution on flotation kinetics of Turkish sphalerite*, Transactions of the Institution of Mining and Metallurgy Section C: Mineral Processing and Extractive Metallurgy 113, 53-59.
- BOULTON, A., FORNASIERO, D., RALSTON, J., 2001. *A comparison of methods to selectively depress iron sulphide flotation*, In: Proceedings of the 4th UBC McGill International Symposium of Fundamentals of Mineral Processing-Interactions in Minerals Processing. Canadian Institute of Mining, Metallurgy and Petroleum Montreal, 141-152.
- CHAVES, A.P., RUIZ, A.S., 2009. *Considerations on the kinetics of froth flotation of ultrafine coal contained in tailings*, International Journal of Coal Preparation and Utilization 29, 289-297.
- CHEN, J., LI, Y., CHEN, Y., 2011. *Cu-S flotation separation via the combination of sodium humate and lime in a low pH medium*, Miner. Eng. 1, 58-63.
- CHEN, J.H., FENG, Q.M., LU, Y.P., 2000. *Energy band model of electrochemical flotation and its application (I): theory and model of energy band of semiconductor-solution interface*, The Chinese Journal of Nonferrous Metals 10, 240-244. (in Chinese)
- CHEN, J.H., LAN, L.H., CHEN, Y., 2013. *Computational simulation of adsorption and thermodynamic study of xanthate, dithiophosphate and dithiocarbamate on galena and pyrite surfaces*, Mineral Engineering 46-47, 136-143.
- CHEN, J.W., BAO, Z.Y., MEI, Y.P., 2007. *Experimental study on mineral dissolution reaction by microcalorimetry*, Bulletin of Mineralogy, Petrology and Geochemistry 26, 496-497. (in Chinese)
- CHEN, X.M., PENG, Y.J., 2015. *The effect of regrind mills on the separation of chalcopyrite from pyrite in cleaner flotation*, Minerals Engineering 83, 33-43.
- EKMEKÇI, Z., DEMIREL, H., 1997. *Effects of galvanic interaction on collectorless flotation behaviour of chalcopyrite and pyrite*, International Journal of Mineral Processing 52, 31-48.
- ELMAHDY, A.M., FARAHAT, M., HIRAJIMA, T., 2016. *Comparison between the effect of microwave irradiation and conventional heat treatments on the magnetic properties of chalcopyrite and pyrite*, Advanced Powder Technology 27, 2424-2431.
- FORNASIERO, D., EIJT, V., RALSTON, J., 1992. *An electrokinetic study of pyrite oxidation*, Colloids Surf. 1-2, 63-73.
- FUERSTENAU, M.C., MILLER, J.D., KUHN, M.C., 1985. *Chemistry of Flotation*. Society of Mining Engineers, New York.
- GAO, S.L., CHEN, S.P., HU, R.Z., LI, H.Y., SHI, Q.Z., 2002. *Derivation and application of thermodynamic equations*, Chinese Journal of Inorganic Chemistry 18, 362-366. (in Chinese)
- GAUDIN, A.M., 1957. *Flotation*. McGraw-Hill, New York, Chap. 2.

- HAUNG, H.H., MILLER, J.D., 1978. *Kinetics and thermochemistry of amyl xanthate adsorption by pyrite and marcasite*, International Journal of Mineral Processing 5, 241-266.
- HE, S.H., SKINNER, W., FORNASIERO, D., 2006. *Effect of oxidation potential and zinc sulphate on the separation of chalcopyrite from pyrite*, International Journal of Mineral Processing 80, 169-176.
- HU, Y.H., ZHANG, S.L., QIU, G.Z., MILLER, J.D., 2000. *Surface chemistry of activation of lime-depressed pyrite flotation*, Trans. Nonferr. Metals Soc. China 6, 798-803.
- JANETSKI, N.D., WOODBURN, S.I., WOODS, R., 1977. *An electrochemical investigation of pyrite flotation and depression*, Int. J. Miner. Process. 3, 227-239.
- LAN, L.H., CHEN, J.H., LI, Y.Q., LAN, P., YANG, Z., AI, G.Y., 2016. *Microthermokinetic study of xanthate adsorption on impurity-doped galena*, Transactions of Nonferrous Metals Society of China 25, 272-281.
- LEPPINEN, J.O., 1990. *FTIR and flotation investigation of the adsorption of ethyl xanthate on activated and non-activated sulfide minerals*, Int. J. Miner. Process. 3-4, 245-263.
- LI, Y., CHEN, J., KANG, D., GUO, J., 2012. *Depression of pyrite in alkaline medium and its subsequent activation by copper*, Miner. Eng. 26, 64-69.
- LI, Q., QIN, W.Q., SUN, W., QIU, G.Z., 2007. *Calculation of electron structure by density function theory and electrochemical process of surface (100) of FeS₂*, Journal of Central South University of Technology 15, 618-622.
- LI, W.Z., QIN, W.Q., SUN, W., QIU, G.Z., 2007. *Electrodeposition of dixanthogen (TETD) on pyrite surface*, Transactions of Nonferrous Metals Society of China 17, 154-158.
- LIU, X.W., CHEN, J.W., BAO, Z.Y., 2002. *The relation between the dissolution thermokinetics of some minerals and their crystal defects*, Journal of Chinese Electron Microscopy Society 21, 751-752. (in Chinese)
- MAIER, G.S., QIU, X., DOBIAS, B., 1997. *New collectors in the flotation of sulphide minerals: a study of the electrokinetic, calorimetric and flotation properties of sphalerite, galena and chalcocite*, Physicochemical and Engineering Aspects 122, 207-225.
- MELLGREN, O., 1966. *Heat of adsorption and surface reactions of potassium ethyl xanthate on galena*, Transactions Society of Mining Engineers 235, 46-59.
- MONTALTI, M., FORNASIERO, D., RALSTON, J., 1991. *Ultraviolet-visible spectroscopic study of the kinetics of adsorption of ethyl xanthate on pyrite*, Journal of Colloid and Interface Science 143, 440-450.
- MOSLEMI, H., GHARABAGHI, M., 2017. *A review on electrochemical behavior of pyrite in the froth flotation process*, Journal of Industrial and Engineering Chemistry 47, 1-18.
- MU, Y.F., PENG, Y.J., LAUTEN, ROLF A., 2016. *The depression of pyrite in selective flotation by different reagent systems- a literature review*, Minerals Engineering 96-97, 143-156.
- MURPHY, R., STRONGIN, D.R., 2009. *Surface reactivity of pyrite and related sulfides*, Surface Science Reports 64, 1-45.
- OWUSU, C., ABREU, S.B.E., SKINNER, W., ADDAI-MENSAH, J., ZANIN, M., 2014. *The influence of pyrite content on the flotation of chalcopyrite/pyrite mixtures*, Minerals Engineering 55, 87-95.
- OWUSU, C., ADDAI-MENSAH, J., FORNASIERO, D., ZANIN, M., 2013. *Estimating the electrochemical reactivity of pyrite ores-their impact on pulp chemistry and chalcopyrite flotation behavior*, Advanced Powder Technology 24, 801-809.
- OWUSU, C., FORNASIERO, D., ADDAI-MENSAH, J., ZANIN, M., 2015. *Influence of pulp aeration on the flotation of chalcopyrite with xanthate in chalcopyrite/pyrite mixtures*, International Journal of Mineral Processing 134, 50-57.
- PENG, Y.J., GRANO, S., FORNASIERO, D., RALSTON, J., 2003. *Control of grinding conditions in the flotation of chalcopyrite and its separation from pyrite*, International Journal of Mineral Processing 69, 87-100.
- QIN, W.Q., LONG, H.Z., QIU, G.Z., SUN, S.Y., 1996. *Surface characteristics and activation of pyrite in high alkaline and calcium medium*, Nonferrous Metals 48, 35-38. (in Chinese)
- QIU, X.H., YU, Y., ZHANG, C.J., 2016. *Flotation kinetics of chalcopyrite and pyrite in tannic acid system*, Chemical Industry and Engineering Progress 35, 2258-2262. (in Chinese)
- RAO, S.R., LEJA, J., 2004. *Surface Chemistry of Froth Flotation*. Kluwer Academic/ Plenum Publishers, New York.
- SHEN, W.Z., FORNASIERO, D., RALSTON, J., 1998. *Effect of collectors, conditioning pH and gases in the separation of sphalerite from pyrite*, Miner. Eng. 2, 145-158.
- SUN, W., ZHANG, Y., QIN, W.L., HU, Y.H., 2010. *Activated flotation of pyrite once depressed by lime*, Journal of Central South University (Science and Technology) 41, 813-818. (in Chinese)
- SUN, X.J., GU, G.H., LI, J.H., HU, Y.H., 2010. *Influences of collector CSU31 on chalcopyrite and pyrite flotation*, Journal of Central South University (Science and Technology) 41, 406-410. (in Chinese)

- WARK, I.W., COX, A.B., 1934. *Principles of flotation, I. An experimental study of the effect of xanthates on contact at mineral surfaces*, Trans. AIME, 112: 189-232.
- WOODS, R., 2003. *Electrochemical potential controlling flotation*, Mineral Engineering 72, 151-162.
- YANG, Q., CHEN, S.P., XIE, G., LIU, X.L., LIU, M.Y., ZHU, Z.L., JIA, Q.S., GAO, S.L., 2014. *Development and application of RD496 microcalorimeter*, Scientia Sinica Chimica 44, 889-914. (in Chinese)
- ZHANG, H.J., LIU, J.T., CAO, Y.J., WANG, Y.T., 2013. *Effects of particle size on lignite reverse flotation kinetics in the presence of sodium chloride*, Powder Technology 246, 658-663.
- ZHANG, Y., QIN, W.L., SUN, W., HE, G.Y., 2011. *Electrochemical behaviors of pyrite flotation using lime and sodium hydroxide as depressants*, The Chinese Journal of Nonferrous Metals 21, 675-679. (in Chinese)
- ZHANG, Y.H., CAO, Z., CAO, Y.D., SUN, C.Y., 2013. *FTIR studies of xanthate adsorption on chalcopyrite, pentlandite and pyrite surfaces*, Journal of Molecular Structure 1048, 434-440.